Optimal Silane Concentration for Strengthening PA12 and SFO Composite Filaments in FDM Printing: Preliminary Insights

Kiran Poudel[1], Oluwasola K. Arigbabowo[1,2], Pratik Karkhanis[1], Wilhelmus Geerts[2,3] & Jitendra Tate[1,2,*]

Texas State University

601 University Drive, San Marcos, TX,78666

[1] Ingram School of Engineering

[2]Materials Science Engineering and Commercialization Program

[3]Department of Physics

*jt31@txstate.edu

Abstract

Silane Treatment is a type of surface treatment which involves the application of silane, a coupling agent on the surface of a material to improve surface adhesion and bonding. Magnetic powder, i.e., Strontium ferrite (SFO), was treated with varying concentrations of silane using different mixing experimental setups. The treated samples were characterized using Thermogravimetric analysis (TGA), X-ray photoelectron spectroscopy (XPS), Scanning electron microscopy (SEM) and Vibrating sample magnetometer (VSM). The silane retention was confirmed by EDAX and the mixing treatment to get a homogeneous distribution of silane on surface of the SFO powder was optimized. XPS measurements suggest the presence of approximately 1 monolayer of silane on the SFO particles. The magnetic properties of the non-treated and treated SFO powders were compared and no change in the magnetization was observed. Following the treatment, 10 wt. % PA-12/SFO filament were manufactured by a twin-screw extruder. Preliminary 3D printing experiments of mechanical test samples show that the flowability of the silane treated filament differs from the untreated material.

Keywords: Silane treatment, Twin Screw Extrusion, Bonded magnets

1. Introduction

Bonded magnets are produced by binding magnetic powders with polymers usually by extrusion or molding processes. Ferrite powders and rare earth magnetic materials are usually bonded with polymers and injection molding is widely used for manufacturing the complex shaped bonded magnets via in-mold magnetization and pulse magnetization methods [1]. They provide design flexibility and are easy on prototyping compared to sintered magnets. Although the magnetic strength of bonded magnets is lowered as compared to other traditional manufacturing methods like sintering because of the porosity and the dilution of the magnetic density due to the polymer matrix, near net-shape magnets with complex magnetic pole distributions can be produced by

injection molding or FDM. Through the use of lubricants and additives it is possible to increase the magnetic loading level and improve the magnetic density [2]. FDM fabrication of magnets brings a wide range of applications to actuators, sensors, and automotive parts.

Nano and microscale magnetic particles exhibiting hard-magnetic properties, can be filled into polymer plastics to bond and form bonded magnets. Hard magnetic materials retain their magnetic properties after the removal of an external magnetic field and have a significant magnetic hysteresis. Only a limited set of materials exhibit significant magnetic moments at room temperature. This group includes elemental iron, nickel, and cobalt, as well as compounds composed of these elements, compounds that contain oxygen, carbon, sulfur and boron or some rare earth elements like neodymium and samarium. Additionally, a few other materials like chromium dioxide, gadolinium metal at temperatures below 20 °C, and various manganese compounds (MnBi, MnSb, MnAs, MnB, Au2MnAl, and Cu2MnAl) also possess substantial magnetic properties. In contrast, most materials have small magnetic moments at room temperature, and their magnetic characteristics become evident only under specialized conditions [3]. Neodymium-Iron-Boron, Samarium-Cobalt, Aluminum-Nickel-Cobalt, Barium Ferrite and Strontium Ferrite are well-known examples of common hard magnetic materials used in permanent magnets.

Lagorce and Allen [4], created magnetic polymer composites, which are compatible with microelectronics and micromachining processes, by using a polyamide as the matrix material and incorporating SFO powder as magnetic filler. These composites demonstrate desirable hard magnetic properties, including square magnetization curves. For samples comprising 80% SFO by volume, they exhibit a high coercivity of approximately 320 kA/m, a residual induction of around 0.3 T, and a maximum energy product of 11900 TA/m (J/m^3). The tensile and flexural strength of these composites are like those of the polyamide, with residual stresses at a level comparable to neat polyimide, and a slightly higher Young's modulus.

Many literatures are available highlighting the improvements in mechanical properties of plant-based fiber composites with thermosets manufactured through traditional manufacturing processes when fibers are silane treated. The silane improves the adhesion between the fibers and the polymer improving the composites strength. R. Kirubagharan1 et al., 2022 [5] observed improvement on mechanical and fatigue behavior of maize husk fiber epoxy composites via alkali-silane treatment. Similarly, M Ramesh et al., 2022 [6] examined the impact of silane treatment on the analysis of composites made from Ipomoea staphylina plant fibers and an epoxy matrix and found improvements in tensile and flexural strengths.

Boon and Mariatti, 2014 [7] examined effects of silane treatment on epoxy thin-film composite filled with magnetite. The silane treated composite showed improvements in saturation magnetization, storage modulus, and glass transition temperature compared to the untreated composite. SJ park et al.,[8] treated glass fibers with silane coupling agents and composites were manufactured in unsaturated polyester resin, they observed increase in surface free energy and mechanical properties. This was attributed to the hydrogen bond between glass fiber and matrix at the composite interface.

Overall, the properties of the composites are improved by application of silane coupling agents on various organic fibers, glass fibers and other inorganic materials. Most of the studies and improvements of properties are observed on thermoset resins and manufactured through manufacturing methods like compression molding and injection moldings. Due to their complexity and cost, for low production volumes traditional methods are less favorable when compared to additive manufacturing (AM). As a result, there is a growing interest in extensive research in the field of creating polymer composites with magnetic particles specifically for 3D printing applications. Campen et al., [9] 3d printed a NdFeB filler and polyoxymethylene matrix composite filament and highlighted the ease of prototyping via FDM. Researchers are exploring several types of fillers and reinforcements to further enhance the performance of these composites. This motivated us to see if the silane coupling on inorganic magnetic powders upon thermoplastic matrix could improve the bonding and overall strengths. To our knowledge this paper is the first report on performing silane surface treatments on SFO fillers for creating high quality magnetic polymer composite filaments with polyamide 12 (PA12) matrix for FDM.

2.Materials and methods

2.1 Materials

2.1.1 Polyamide 12 (PA 12)

Polyamide 12 (PA12) has lower impact resistance but exhibits good resistance to abrasions and UV radiation. It also has a lower water absorbency compared to other polyamide types. PA12 has good dimensional stability and reasonable electrical properties. Furthermore, it is well-suited for applications where safety, durability, or long-term reliability is needed. Transparent grades of PA12 are available, providing flexibility in terms of design and creation.[10] It is derived from monomers called aminolauric acid or laurolactam, which consist of 12 carbon atoms each. PA12 is formed by polymerization of a diamine and a diacid, commonly by condensation polymerization of laurolactam, which is a cyclic amide monomer. In this process, laurolactam undergoes ring-opening polymerization, where the lactam ring is opened by the amine functional group of the monomer. The resulting polymer chain contains repeated monomer chains of amide, creating the polyamide structure of PA12. PA12 from

Evonik Corporation is used in this study as they have good mechanical and chemical performance for FDM.

2.1.2 Strontium Ferrite (SFO)

The SFO powder is a type of magnetic powder composed of strontium, iron, and oxygen. SrFe12O19 is a hexaferrite, a ceramic hard magnetic ferrite that has a hexagonal structure composed of strontium iron oxide. This ferrite is known for its ability to withstand demagnetizing fields and retain its magnetization in zero field, as well as their cost-effectiveness and lower material requirements compared to the more expensive NdFeB and SmCo magnets. Additionally, they exhibit excellent chemical stability and high resistance to corrosion, which contributes to the longevity and durability of components made from these materials [11]. Furthermore, enhancement in their magnetic properties can be achieved by modifying them to micro and nanoscale sizes [12].

SFO particles used in this study are provided by Dowa Electronics Materials Co. Table 1 shows the properties OP-56 which was used as filler material in the magnetic composite in this experiment.

Table 1. Properties of OP-56 powders [13]

Descriptions	Powder's Properties		Magnetic Properties - Compress Method			Magnetic Properties - Calender Roll Molded				
	Average Particle Diameter (APD)	Compressed Density (CD)	Residual Induction (Br)	Coercive Force (HcB)	Intrinsic Coercive Force (HcJ)	Density of Pressing (Dp)	Residual Induction (Br)	Coercive Force (HcB)	Intrinsic Coercive Force (HcJ)	Maximum Energy Product ((BH)max)
Unit SI / cgs / Products	μm / —	g/cm^3 / —	mT (G)	kA/m (Oe)	kA/m (Oe)	g/cm^3 / —	mT (G)	kA/m (Oe)	kA/m (Oe)	kJ/m^3 (MGOe)
OP-56	1.05±0.15 / —	3.10±0.1 / —	190±7 (1900±70)	130±8 (1630±100)	250±16 (3200±200)	3.54	249 (2490)	181 (2280)	264 (3320)	11.7 (1.47)

2.1.3 Silane

Silane are coupling agents with bifunctionality and are widely used as adhesion promoter. Fig 1 shows the basic silane structure of silanes with an organofunctional group(Y) on the left which will bond with polymers and resins, and a silicon functional group on the right which will bond with fillers. Tri chloro and Tetra chloro silicon are reacted with alcohol to form the liquid silane and undergo nucleophilic substitution to get functionality.

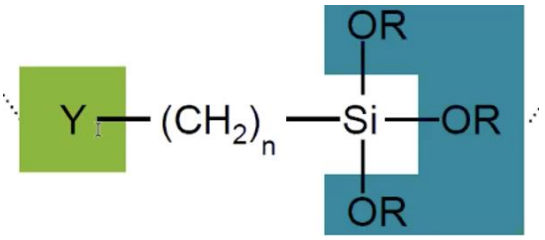

Figure 1. Silane structure 14]

VPS 2978 silane, which is provided by Evonic Industries, was used for this research. Its nontoxic nature and higher thermal stability make it suitable for our purpose. The organic part of VPS 2978 comprises of benzene ring, amine functional group and vinyl chain, which will bond with PA12 in our research and is the first to undergo degradation. The functionality on the inorganic side is –OH in VPS 2978 alongside silicon. This will bond with strontium ferrite in our experiment. It is a colorless, liquid, amino silane with –OH functional group and is a water dilution silane.

2.2 Silane treatment

Since the goal of the research is the fabrication of high-quality filaments with improved strength, the focus here was on the formation of a silane monolayer on the surface of the SFO powder. The silicon functional group of the VPS 2978 will bond with the OH groups present on the SFO surface to make a strong covalent bond. The organofunctional group will have a polar hydrogen bond with PA12 during filament fabrication. Since the silane - ferrite bond is much stronger than the silane - silane bonding, the target is to achieve a single layer of coating around the strontium ferrite powders. The theoretical monolayer thickness is calculated to be 2.44nm, calculated based on the wetting area of OP56 and the specific volume of silane. Although it is not possible to quantify the silane layer on our research scale, the correct amount silane input and homogeneous distribution of elements like Nitrogen and silicon will affirm our proximity to monolayer [14].

One hundred ml of water was added to 50 g of SFO and 1.29 gram of silane to make a slurry. The mixture was stirred with a glass rod so that the silane is properly distributed through the suspension. The mixture was sonicated with a Sonics and Materials, Inc., VCX 750 sonicatior. After the sonication was done, the samples were dried in a vacuum oven at 120°C for 2 hours and then the samples were sealed to protect from ambient moisture.

2.2.1Probe sonication mixing:

The amount of silane required to form a single monolayer on the SFO was estimated from the weight of the SFO, the specific area of OP-56 SFO, and the mass densities of OP-56 and VPS 2978. A single monolayer would require adding approximately 1 wt. % of VPS2978 to the SFO

powder. The effect of 4 different surface treatments was explored. The samples were prepared without sonication, 4.5 mins of sonication, 4.5 mins of sonication and rinsing, and 9.5 min sonication. The probe sonication method was applied without any additional attachments. The literature suggested that the 8400 J was the optimal energy for mixing [15]. A higher energy can bring particle collisions and may cause re- agglomeration. The sonicator was brought in contact with the fluid above the sedimented SFO particles. The proximity to the SFO particles resulted in better dispersion and so during the treatment the probe was adjusted such that it vibrates the entire liquid surface without touching the SFO solid particles. The setup shown in figure 2 was used for sonication of silane, SFO, and water slurry.

Figure 2. Probe sonication mixing

2.2.2. Drying and Dehydration:

Following the sonication, the surface treated slurry was spread out on an aluminum foil and dried in a furnace. The area the slurry is spread out on should be maximized to improve drying efficiency. The dehydration was done for 2 hours at 120°C. During this process the water in the slurry evaporates and thus, silane was bonded to the surface of SFO-oxide.

2.3 Filament fabrication

Two different composite filaments were fabricated at 10 wt. % of filler loading with silane treated SFO. The PA12 was dried at 50°C for a week before the extrusion. A Fisher scientific extruder with co-rotating twin screws housed by cylindrical barrel was used for the composite filament fabrication. The matrix and filler materials were feed via a hopper connected to the barrel and twin-screw extruders provided required shear, mixing and flow along with the varying temperature zones at the barrel. Filaments were compounded under the maximum torque of 7.5 Nm while matrix and feeders were fed at 73rpm and 9rpm. The temperature zones from the feeder to die were 220 °C,220 °C,200 °C,215 °C,210 °C,195 °C and 190°C. Water bath cooling was used for rapid cooling and solidification of the filament. The filament was fabricated at 1.75 ± 0.05mm diameter and spooled afterwards. The setup is displayed in Fig. 3 below.

Fig 3: Fisher scientific twin screw extruder

2.4 3D printing

3D printing was done with 10wt% SFO/PA12 filaments with and without silane surface treatment performed on the SFO particles. The silane treated filaments had a lower flow rate than the filaments with silane treatment causing issues like wrapping and nozzle clogging. The printing difficulties lead to the realization that a bigger nozzle size or a different nozzle material could mitigate this issue. This work will be continued as part of the research.

3. Material characterization

3.1 Thermogravimetric analysis

TGA analysis was performed to observe the weight change with respect to increase in temperature. The silane treated SFO loses moisture at first then the degradation starts around 310°C and finally the residue is inorganic part of the silane bonded to SFO.

TGA was performed on TA Discovery SDT 650 on an alumina pan. TGA was performed by removing the moisture and contamination isothermally at 120 °C. The samples were ramped at 10 °C/min before equilibrating at 120°C. Following the isothermal exchange for 10 mins, it was again ramped up to 750 °C at 10 °C/min.

3.2 Scanning electron microscopy

In the silane treated samples, it is important to verify the uniformity of dispersion and bonding of silane over the surface of SFO powders. The Axia chemi scanning electron microscopy (SEM) was used to quant map the surface of treated powder samples. The silicon and Nitrogen from inorganic and organic functionality of silane respectively, were mapped to see the uniformity of distribution post treatment.

3.3 X-ray photoelectron spectroscopy

Silane treatment being a surface phenomenon, to observe the elemental composition at the surface of the silane treated powder sample, Thermofisher Nexa X-ray Photoelectron Spectroscopy (XPS) was used. XPS measures the energy of emitted electrons to determine the elemental composition and chemical state of a material's surface.

3.4 Magnetic Characterization

A MicroSense EZ9 Vibrating sample Magnetometer (VSM) was used to measure the magnetic properties of the not treated and surface-treated SFO powders. Prior to loading the powder, its mass was measured with a Cahn30 microscale balance down to 1 ugram. The powder was inserted in a custom design powder holder. Although the powder was compacted in the plastic holder no binding agent was used. It is to be expected that the strontium-ferrite platelets are predominantly oriented in the holder with their c-axis (easy axis) perpendicular to the magnetic field.

4. Results and Discussions

4.1 Optimal silane treatment methodology

The TGA on 4 samples prepared at varying sonication times were compared and the results are shown in Fig. 4 below. Several steps can be observed in the TGA graph. The one around 120^{o}C is related to the evaporation of water. The organic part of the silane starts to degrade around 310 and will be fully combusted at 700^{o}C. The total weight loss from 310 to 700^{o}C was used to estimate the amount of silane in the sample. The surface treated sample sonicated for 4.5 mins had the most silane, so its silane retention was maximum. The weight % change and silane retention comparison are summarized in Table 2. Rinsing with water appears to slightly lower the silane retention.

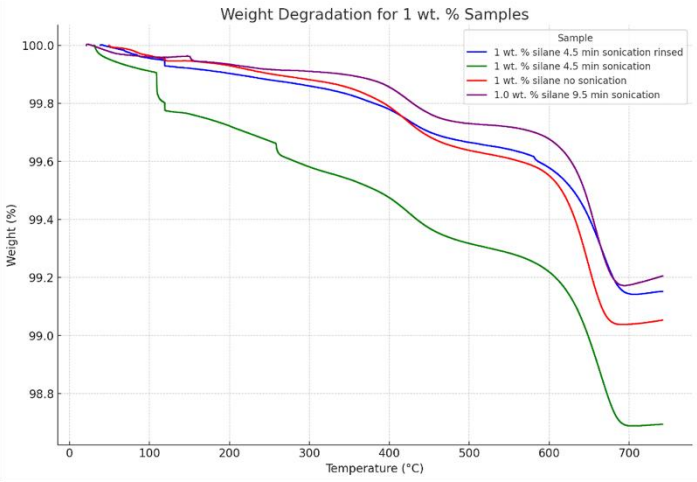

Fig 4: TGA degradation of 1 wt. % silane samples at different sonication times

Table 2: Silane retention comparison between 1 wt.% samples

Sample	Silane retention %
1 wt. % silane (9.5min sonication)	73.6
1 wt. % silane (4.5min sonication)	88.0
1 wt. % silane (No sonication)	71.3
1 wt. % silane Rinsed before drying (4.5min sonication)	83.9

Although the silane retention on the 4. 5 min sonicated sample is better compared to the other samples, it is important to verify the uniform distribution of silane on the SFO surface. EDAX measurements were performed in a SEM on the samples. Figures 5 and 6, show that Nitrogen and silicon were detected and are present through the powder. As most of the powder contributes to the EDAX signal and the silane is just at the surface of the SFO particles, EDAX might not be sensitive enough to detect the distribution of the thin silane layer.

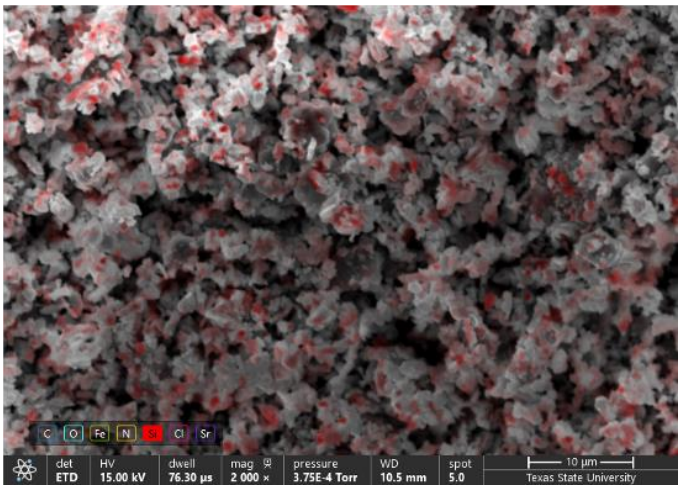

Fig 5: Silicon mapping for 1 wt.% 4.5 min sonication sample

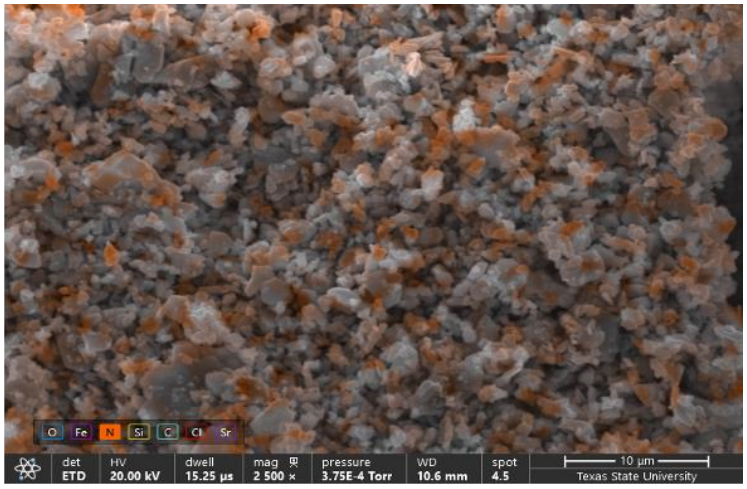

Fig 6: Nitrogen mapping for 1 wt.% 4.5min sonication samples

XPS, a more surface sensitive method (1.5-4 nm), was also used to measure the silane layer on the SFO surface. Table 3 obtained with XPS, confirms the presence of all the peaks coming from VPS 2978 and the SFO. As large SFO peaks were measured the VPS2978 film was thinner than XPS photoelectron escape depth which for oxides is between 1.5 and 4 nm. Assuming the silane layer is continuous, the XPS data confirms that its thickness is approximately 2.75 nm which is approximately a monolayer.

Table 3: Elemental peak table for 1 wt.% silane treated samples 4.5 mins sonication

Peak	**Binding energy eV**	**Atomic wt. %**
Si 2s	153.36	3.55
Cl 2p	198.87	0.73
C 1s	285.28	30.52
N 1s	399.87	4.03
O 1s	530.12	29.9
Sr 3d	133.97	1.29
Fe 2p1	724.04	5.75
Fe LM2	785.06	24.24

4.2 Magnetic performance

The hysteresis loop was measured between –2.2 T to 2.2 T with the VSM at a sweep rate of 400 Oe/sec. The raw data was corrected for the field lag and image effect and normalized on the mass of the sample. The normalized values of saturation of the magnetization suggests that the silane

treatment had no measurable effect on the magnetization. The small change in Mr between both curves is caused by a different orientation of the particle in the powder sample-holder so caused by the loading of the powder. Figure 7 shows the hysteresis loops of the 1 wt.% silane treated SFO and as received non-treated SFO.

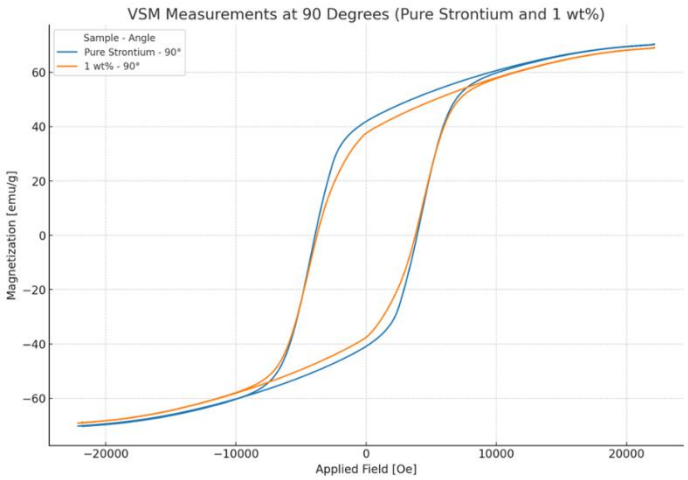

Fig 7: Hysteresis measurement comparison of silane treated and untreated sample

5. Conclusion

Composite filament with 10 wt.% loading level of silane treated SFO and PA12 were successfully fabricated. The final diameter of the composite filament was 1.75± 0.05mm and suitable for FDM printing. Silane treatment was completed by sonication mixing and successive drying process. Based on silane retention, mapping, and spectroscopy results, 1 wt.% of silane to SFO is found to be optimal amount of silane input for the sonication mixing. The sonication time of 4.5 minutes at 40% amplitude ensured the perfect timing maximizing the dispersion as well as avoiding agglomeration.

Normalized magnetic measurement values compared pre and post silane treatment suggested the retention of magnetic properties of SFO. The future work on FDM printing of the composite filament followed by mechanical tests are scheduled to determine the impact of the silane treatment on the mechanical properties of 3D printed test samples.

6. Acknowledgment

This work was supported in part by NSF through DMR-MRI Grant under awards 2216440 and in part by DOD instrumentation grant (78810-W911NF-21-1-0253).

The authors would also like to thank Gregory Treich (senior scientist, Evonik Industries), Advanced Composite Lab (ACL), Optical Characterization Lab, Advance Prototyping Lab & Shared Research Operations (SRO) at Texas State University.

References

[1] T. Schliesch, "Injection molded permanent magnets," in *Modern Permanent Magnets*, J. Croat, and J. Ormerod, Eds. Woodhead Publishing Series in Electronic and Optical Materials, Woodhead Publishing, 2022, pp. 209-250. doi: 10.1016/B978-0-323-88658-1.00009-1.

[2] Damnjanović and N. Kovačević, "Influence of Magnet Particle Shape on Magnetic and Environmental Stability of FDM Polymer-Bonded Magnets," Materials, vol. 16, no. 2993, 2023. [Online]. Available: https://doi.org/10.3390/ma16082993

[3] J. N. Anker and T. Mefford, Biomedical applications of magnetic particles, First edition. ed. CRC Press, 2021.

[4] L. K. Lagorce and M. G. Allen, "Magnetic and mechanical properties of micromachined SFO/polyimide composites," Journal of Microelectromechanical Systems, J. Microelectromechanical Systems, Journal of, J. Microelectromech. Syst., Periodical vol. 6, no. 4, pp. 307-312, 12/01/ 1997, doi: 10.1109/84.650127.

[5] R. Kirubagharan, S. Dhanabalan, and T. Karthikeyan, "Effect of optimized alkali-silane treatment on mechanical and fatigue behavior of maize husk fiber epoxy composites: a strength factor approach," Biomass Conversion and Biorefinery: Processing of Biogenic Material for Energy and Chemistry, Original Paper pp. 1-9, 12/20/ 2022, doi: 10.1007/s13399-022-03661-0.

[6] M. Ramesh, L. Rajeshkumar, C. Deepa, M. Tamil Selvan, V. Kushvaha, and M. Asrofi, "Impact of Silane Treatment on Characterization of Ipomoea Staphylina Plant Fiber Reinforced Epoxy Composites," Journal of Natural Fibers, Article vol. 19, no. 13, pp. 5888-5899, 2022, doi: 10.1080/15440478.2021.1902896.

[7] M. S. Boon and M. Mariatti, "Silane treatment of magnetite filler and its effect on the properties of magnetite-filled epoxy thin-film composites," Polymer Bulletin, Original Paper vol. 71, no. 12, pp. 3333-3346, 12/01/ 2014, doi: 10.1007/s00289-014-1253-8.

[8] S. J. Park, J. S. Jin, and J. R. Lee, "Influence of silane coupling agents on the surface energetics of glass fibers and mechanical interfacial properties of glass fiber-reinforced composites," *Journal of Adhesion Science and Technology*, vol. 14, no. 13, pp. 1677–1689, 2000. doi: 10.1163/156856100742483.

[9] K. von Petersdorff-Campen, Y. Hauswirth, J. Carpenter, A. Hagmann, S. Boës, M. Schmid Daners, D. Penner, and M. Meboldt, "3D Printing of Functional Assemblies with Integrated

Polymer-Bonded Magnets Demonstrated with a Prototype of a Rotary Blood Pump," Appl. Sci., vol. 8, no. 1275, pp. 1-10, Aug. 2018. DOI: 10.3390/app8081275.

[10] "Polyamide (PA) Nylon," Special Chem, 2024. [Online]. Available: https://omnexus.specialchem.com/selection-guide/polyamide-pa-nylon. [Accessed: 10-Sept-2024].

[11] A. Verma, O. P. Pandey, and P. Sharma, "ChemInform Abstract: SFO Permanent Magnet—An Overview," ChemInform, vol. 32, no. 38, pp. no-no, 09/18/Number 38/September 2001, 2001, doi: 10.1002/chin.200138258.

[12] S. V. Ketov, Y. D. Yagodkin, and V. P. Menushenkov, "Structure and magnetic properties of SFO anisotropic powder with nanocrystalline structure," Journal of Alloys and Compounds, Article vol. 509, no. 3, pp. 1065-1068, 01/01/January 2011, 2011, doi: 10.1016/j.jallcom.2010.09.184.

[13] DOWA HD Corporation, "Home," 2024. [Online]. Available: https://hd.dowa.co.jp/en/index.html. [Accessed: 10-Sept-2024].

[14] Evonik Industries AG, "Corporate U.S.," 2024. [Online]. Available: https://corporate.evonik.us/en. [Accessed: 10-Sept-2024].

[15] Crandon et al., (2019). Sonication energy for the preparation of aqueous nanoparticle dispersions. Journal of Engineering Research and Application,